ARMY RESEARCH LABORATORY

The Influence of Flow Dispersers on 30-mm Gun-Type Annular Jets— XM46 Combustion and Flash X-ray Photography of Aqueous NaI Solutions

Avi Birk
Michael McQuaid
Matthew Cross

ARL-TR-720 April 1995

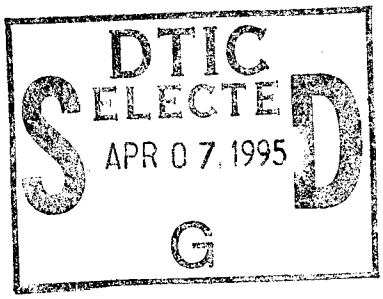

NOTICES

Destroy this report when it is no longer needed. DO NOT return it to the originator.

Additional copies of this report may be obtained from the National Technical Information Service, U.S. Department of Commerce, 5285 Port Royal Road, Springfield, VA 22161.

The findings of this report are not to be construed as an official Department of the Army position, unless so designated by other authorized documents.

The use of trade names or manufacturers' names in this report does not constitute endorsement of any commercial product.

REPORT DOCUMENTATION PAGE

Form Approved
OMB No. 0704-0188

1. AGENCY USE ONLY *(Leave blank)*	2. REPORT DATE	3. REPORT TYPE AND DATES COVERED
	April 1995	Final, Nov 93 - Nov 94

4. TITLE AND SUBTITLE

The Influence of Flow Dispersers on 30-mm Gun-Type Annular Jets--XM46 Combustion and Flash X-ray Photography of Aqueous NaI Solutions

5. FUNDING NUMBERS

4G592-562-R3-203R

6. AUTHOR(S)

Avi Birk, Michael McQuaid, and Matthew Gross

7. PERFORMING ORGANIZATION NAME(S) AND ADDRESS(ES)

U.S. Army Research Laboratory
ATTN: AMSRL-WT-PA
Aberdeen Proving Ground, MD 21005-5066

8. PERFORMING ORGANIZATION REPORT NUMBER

ARL-TR-720

9. SPONSORING/MONITORING AGENCY NAMES(S) AND ADDRESS(ES)

10.SPONSORING/MONITORING AGENCY REPORT NUMBER

11. SUPPLEMENTARY NOTES

12a. DISTRIBUTION/AVAILABILITY STATEMENT

Approved for public release; distribution is unlimited.

12b. DISTRIBUTION CODE

13. ABSTRACT *(Maximum 200 words)*

This report summarizes an experimental study to characterize the influence of the injector exit configuration on the flow and combustion dynamics of regeneratively injected XM46. In particular, it identifies differences in the spray structure and combustion dynamics produced when a 60° wedge flow disperser is attached to a "basic" injector configuration. The study consisted of two parts. The first part involved characterizing the structure of aqueous sodium iodine (NaI) sprays via flash x-ray and scattered visible light photography. NaI solutions were injected at velocities ranging from 25 to 76 m/s into nitrogen at 7.6 or 17.2 MPa. It was found that in tests where the flow disperser was not used, the sprays tended to collapse and concentrate along the chamber centerline. When the flow disperser was employed, the liquid scattered away from the center, and a more uniform distribution of the liquid was produced in the chamber.

In the second part of this study, XM46 sprays were ignited in the combustion products of $O_2/H_2/Ar$ gas mixtures. The intial chamber pressure was 9–10 MPa, and the XM46 combustion elevated chamber pressures into the range of 30–45 MPa. Pressure oscillations developed at peak combustion pressures when the basic injector configuration was employed, but not when the flow disperser was attached. These results, coupled with the results from the flash x-ray experiments, suggest that the pressure oscillations are attributable to the spontaneous ignition of poorly dispersed blobs of XM46. The results are discussed with respect to the large pressure spikes occasionally observed during the puddle ignition startup of the ATD 155-mm regenerative liquid propellant gun (RLPG) fixture.

14. SUBJECT TERMS

liquid propellant guns, spray combustion, x-ray imaging of sprays, flow, injectors

15. NUMBER OF PAGES

24

16. PRICE CODE

17. SECURITY CLASSIFICATION OF REPORT	18. SECURITY CLASSIFICATION OF THIS PAGE	19. SECURITY CLASSIFICATION OF ABSTRACT	20. LIMITATION OF ABSTRACT
UNCLASSIFIED	UNCLASSIFIED	UNCLASSIFIED	UL

INTENTIONALLY LEFT BLANK.

TABLE OF CONTENTS

INTENTIONALLY LEFT BLANK.

LIST OF FIGURES

INTENTIONALLY LEFT BLANK.

1. INTRODUCTION

This report summarizes our most recent experimental study to characterize the dynamics of XM46 spray combustion as it relates to the development of regenerative liquid propellant gun (RLPG) technology. Previously reported studies include (1) visualization of the combustion of thin XM46 sprays produced by injection through a straight-walled, annular exit channel at pressures up to 10 MPa (Birk and Reeves 1987); (2) visualization of LGP1845 spray combustion at 35 MPa following injection through a simple circular orifice (Birk, McQuaid, and Bliesener 1992); and (3) imaging the core structures of thin annular and circular jets produced by injection through a straight-walled channel using flash x-ray photography (Birk, McQuaid, and Gross 1993).

The experimental results reported here are our first to characterize XM46 spray combustion following its injection through an annular exit channel that mimics the channel formed by the inner and outer pistons of a typical 30-mm Concept VIC RLPG injector. The radius of the exit channel wall formed by the outer piston typically decreases, then increases; while the radius of the inner channel wall/piston decreases and produces a truncated conical form which extends into the combustion chamber. Significant resources are being invested in modeling the flow produced by injection through such channels, but the experimental (visualization) data necessary to validate this effort do not currently exist. This deficiency makes it very difficult to design improvements that address RLPG issues. Potential solutions must be investigated by trial and error. For example, significant reductions in pressure oscillations have been achieved in recent ARL 30-mm RLPG gun firings through the use of flow dispersers (DeSpirito et al. 1994). (The dispersers are flow deflectors/splitters mounted as an extension to the conical protrusion of the inner piston.) However, it is not clear why certain dispersers are effective and others are not, and the mechanisms leading to oscillation reduction can only be speculated. Mechanisms that have been proposed include (1) improved propellant dispersion, (2) enhanced turbulent mixing, and (3) disturbance of chamber acoustic modes. The lack of pertinent experimental data that can be used as a basis to design system improvements was the impetus for undertaking the work reported here.

This study involves two parts. The first part characterizes the spray structure of aqueous sodium iodine (NaI) solutions through simultaneously obtained flash x-ray and visible light images. (The NaI solution has a high x-ray absorption cross section.) The sprays were produced by injecting the solutions at velocities ranging from 25 to 76 m/s into 7.6 or 17.2 MPa of nitrogen. The core structures of the jets were revealed through the use of the flash x-ray photography. The second part of this study characterizes

the effect of injector exit configuration on XM46 spray ignition and combustion. In this case, the XM46 was injected into the post combustion products of a spark-initiated mixture of $O_2/H_2/Ar$. High-speed color cinematography was selectively employed to image the spray dynamics and the chamber pressure was recorded. The photographic data obtained were of poor quality, but the (chamber) pressure vs. time traces proved to be very interesting. Pressure oscillations were recorded when the basic injector configuration was employed, but not when the flow disperser was attached. Since the conditions during which the XM46 combusts in our experiments are similar to those during the "puddle" ignition process used to start the regenerative injection process in the AFAS ATD 155-mm gun fixture, the results suggest a mechanism leading to the large pressure spikes occasionally observed during the puddle ignition phase of the interior ballistic cycle. This aspect of the experimental results is the main focus of this report.

2. EXPERIMENTAL SETUP

The two experimental configurations used in this study are shown in Figures 1 and 2. Setup A was used for the XM46 combustion tests, while setup B was used for the x-ray imaging of aqueous NaI sprays. The same regenerative injector (Figure 2) was used in both setups (Birk and Bliesener 1991). The exit channel geometry of the basic injector configuration approximates that of the ARL 30-mm RLPG injector. Tests that compare the dynamics obtained with a basic configuration, and with a "daisy wheel" 60°-wedge-jet-disperser (60WD) attached to the injector centerbolt, were conducted in both setups. Tests with 45WD, CONE, and PINS jet-dispersers were conducted only in setup B. The jet-dispersers shown in Figure 2 are the same ones that were employed by DeSpirito et al. in a 1994 study.

Details of the test chamber used in setup A have been described previously (Birk, McQuaid, and Bliesener 1992). The chamber is a cylindrically shaped vessel with an inner diameter of 76.2 mm. It has four opposing viewing ports that can be equipped with sapphire or Lexan windows. To ignite the XM46 spray, the chamber pressure and temperature were raised by preloading the chamber with 1.12–1.4 MPa of an $O_2/H_2/Ar$ gas mixture. This mixture was ignited with an automotive spark plug. Because the window seals are metal c-rings, which are prone to gas leaks, the $O_2/H_2/Ar$ mixture was premixed in a 2,000-cm^3 leak-proof chamber. This chamber was isolated from the combustion chamber by a remotely controlled pneumatic valve (PV). Five seconds before the injection, the PV was opened and the pressure was allowed to equilibrate between the two chambers. The PV was then closed just before the gas mixture in the chamber was initiated. The preload pressures of the $O_2/H_2/Ar$ mixtures were restricted to

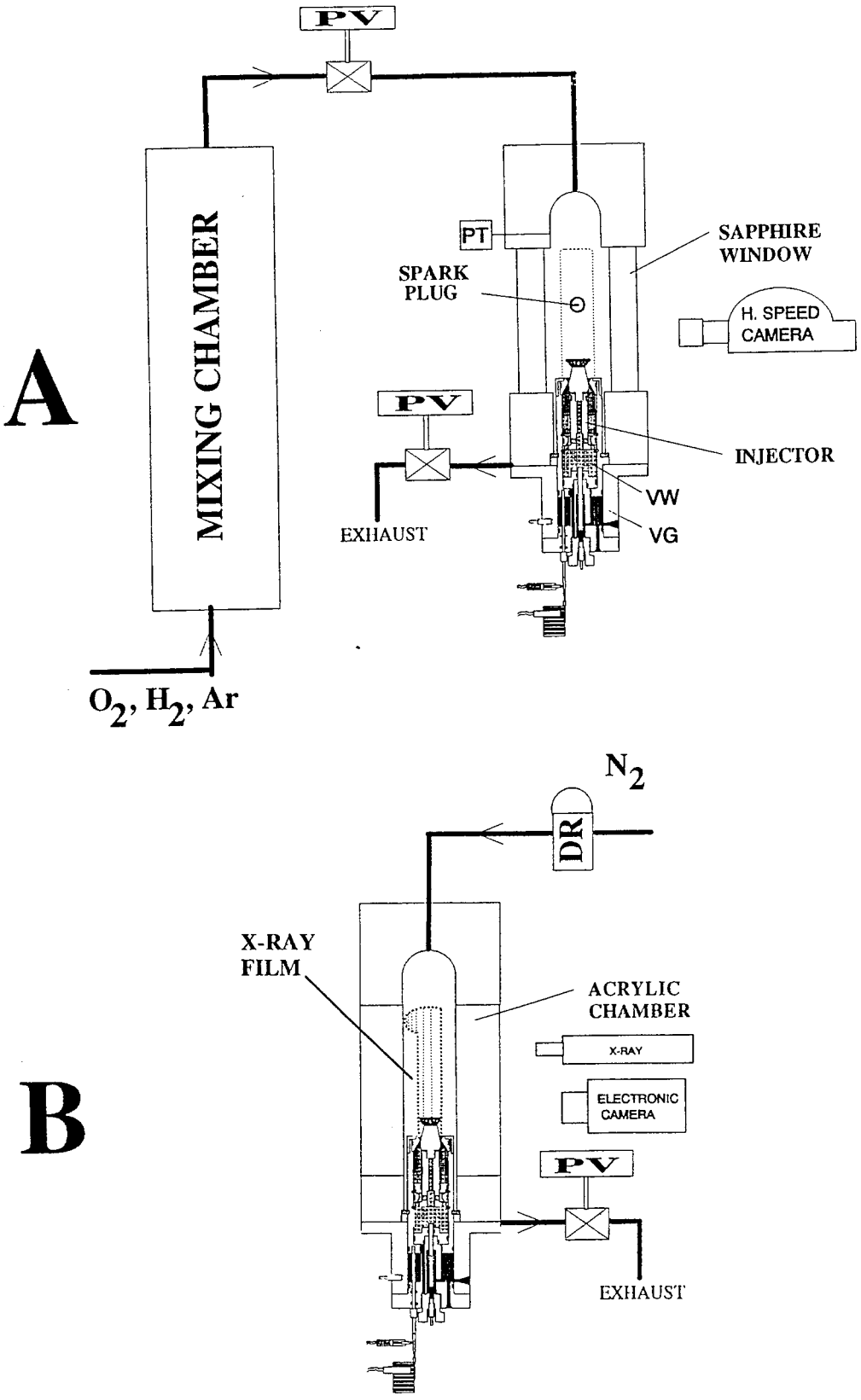

Figure 1. Experimental setup.

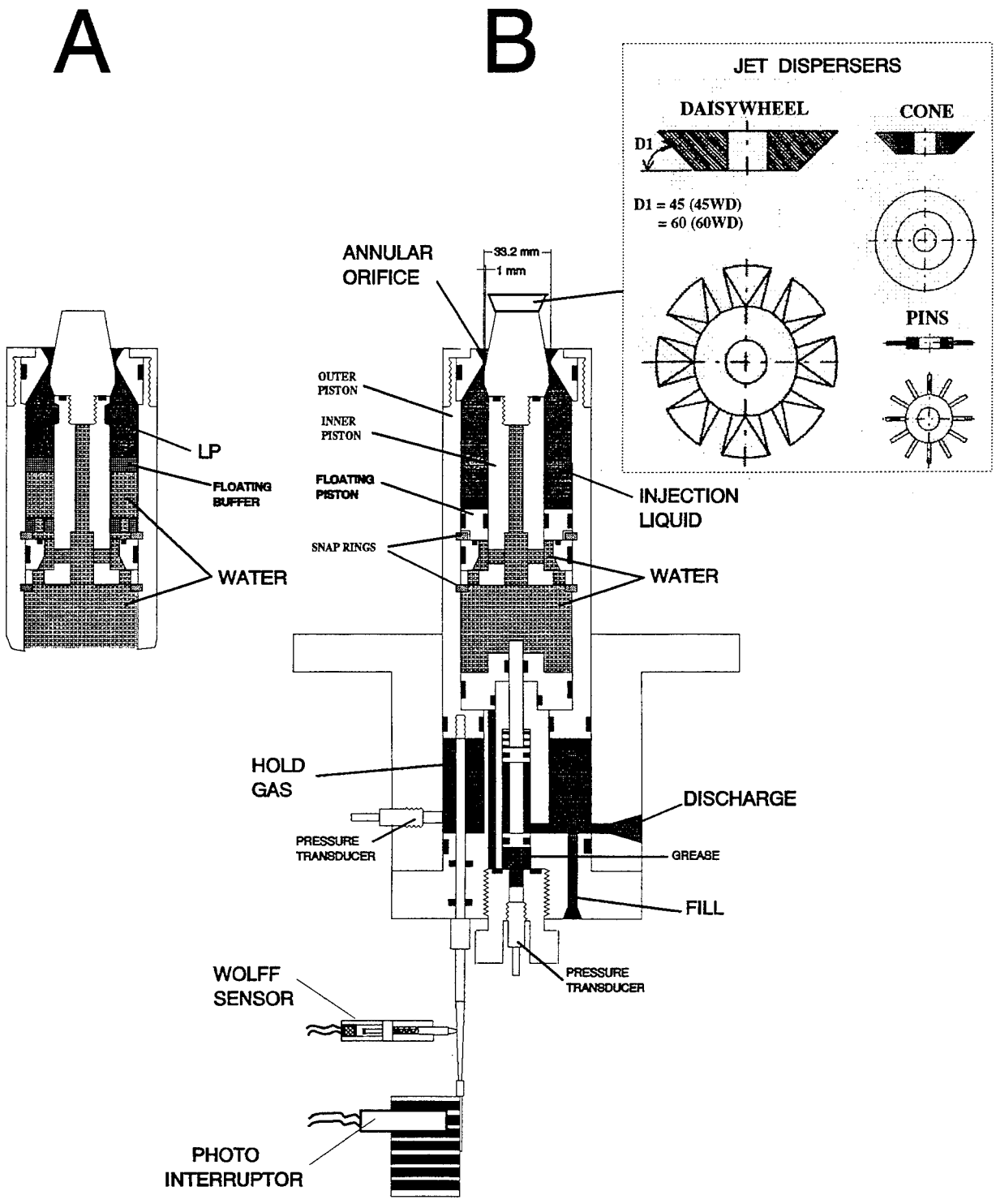

Figure 2. Injector configurations.

the range of 1.12–1.4 MPa by operational considerations. Below 1.12 MPa, the propellant spray failed to ignite reliably. Above 1.4 MPa, the spark plug failed to ignite the $O_2/H_2/Ar$ mixture. Chamber pressures reached 9–10 MPa following ignition of the gas. A Kistler 607L pressure gauge (PT) was used to record the chamber pressure (P_G).

In tests with XM46 (setup A), injection commenced when P_G exceeded a pressure threshold corresponding to the completion of the $O_2/H_2/Ar$ combustion. The propellant and water volumes in the injector were separated by a Teflon ring (the "floating buffer" in Figure 2). As the ring pushes toward the exit channel, its seal with the inner surface fails, allowing water to flush out the remaining XM46. Because of this procedure, a small amount of water was injected into the chamber following the XM46 injection. Before injection, the injector piston assembly extended into the chamber and the gas volume was 825 cm^3. The piston assembly retracts during the injection process and the gas volume following injection was 950 cm^3. Piston motion was monitored with a Wolff sensor and a photo-interrupter device. The latter provided a signal linearly proportional to the piston velocity, and, hence, injection velocity. The output from these devices and the pressure gauges were recorded with a Nicolet Pro 20 waveform recorder.

Setup B was designed to allow flash x-ray photography to be used to study the influence of the injector configuration on the core structure of the sprays. The dense liquid core, which is hidden to standard (scattered visible light) imaging techniques by a high number density shroud of liquid particles, contains the bulk of the unreacted liquid. However, the x-ray technique requires an object (liquid) with a high x-ray absorption cross section, and XM46 is practically transparent to x-rays. Therefore, we chose to inject an aqueous NaI solution, which has the requisite absorption cross section and a density (1.5 g/cm^3) similar to XM46. The technique also requires a chamber (or chamber window) material that is transparent to x-rays. Acrylic was chosen to meet this requirement. Besides having a low x-ray absorption cross section, acrylic is also visibly transparent. Thus, images based on visible light scattering and x-ray photographic techniques could be acquired simultaneously.

The chamber used in setup B consisted of two parts. The top part was borrowed from the setup A chamber, while the center part is a cylinder made from acrylic. The cylinder has a 203-mm OD and a 85-mm ID. Its volume is 20% larger than the setup A chamber. This chamber, which is rated for use up to 10 MPa, was pressurized with nitrogen. The chamber pressure was established and controlled via a dome pressure regulator (DR). Injection is started by discharging the gas from the injector's hold

volume (VG). The test liquid is injected as the water containing volume (VW) acts on the differential area metal ring (i.e., the "floating piston" in Figure 2). The ring serves as a floating buffer between the NaI solution and the water in the injector. It is displaced once the pressure in VG has dropped below a threshold value. Lowering the threshold results in higher injection velocity. A few tests were conducted at higher P_G than possible in the acrylic chamber by using the metal chamber (used in setup A) equipped with a Lexan window.

A high-speed framing camera (Photec) was used to photograph the self-illuminating combustion process obtained in setup A. In tests with setup B, quartz flood lights were used to illuminate the spray for either the framing camera or an electronic camera system (EEV). The EEV is comprised of three CCD cameras and a controller. The cameras are mounted behind beam-splitting optics that enable them to observe the same field of view. The delay times between individual camera triggering and the exposure times are controllable. The first CCD camera was triggered simultaneously with the x-ray (HP 150 keV) by a signal from the photo-interrupter. The x-ray technique and image digitization procedure employed here are very similar to those discussed in Birk, McQuaid, and Gross (1993). The only difference is that the light-tight film/intensifier pack is inside the acrylic chamber and attached to the top of the injector. In this configuration, its shape conforms to the chamber's inner wall.

3. RESULTS

3.1 Visualization Data From the NaI Solution Tests. Images representative of the results obtained when an NaI solution was injected are shown in Figures 3 and 4. Results corresponding to two different chamber pressures are provided. The sprays at an ambient pressure of 7.58 MPa were imaged through the acrylic chamber's walls. Distortion in the original image, due to the curved mounting of the film in the acrylic chamber, has been corrected by an image processing software routine. Figure 5 shows an example of such correction. Images of the sprays at an ambient pressure of 17.24 MPa were taken through a Lexan window in the metal chamber. The visible light images obtained for tests conducted at 17.24 MPa were uninformative—the enhanced atomization at the higher pressure led to visual "white out" of the spray's features.

The x-ray images reveal the core structures of the sprays, with details resolved down to 0.2 mm. They indicate that when the basic injector configuration was employed, the liquid remained attached to the

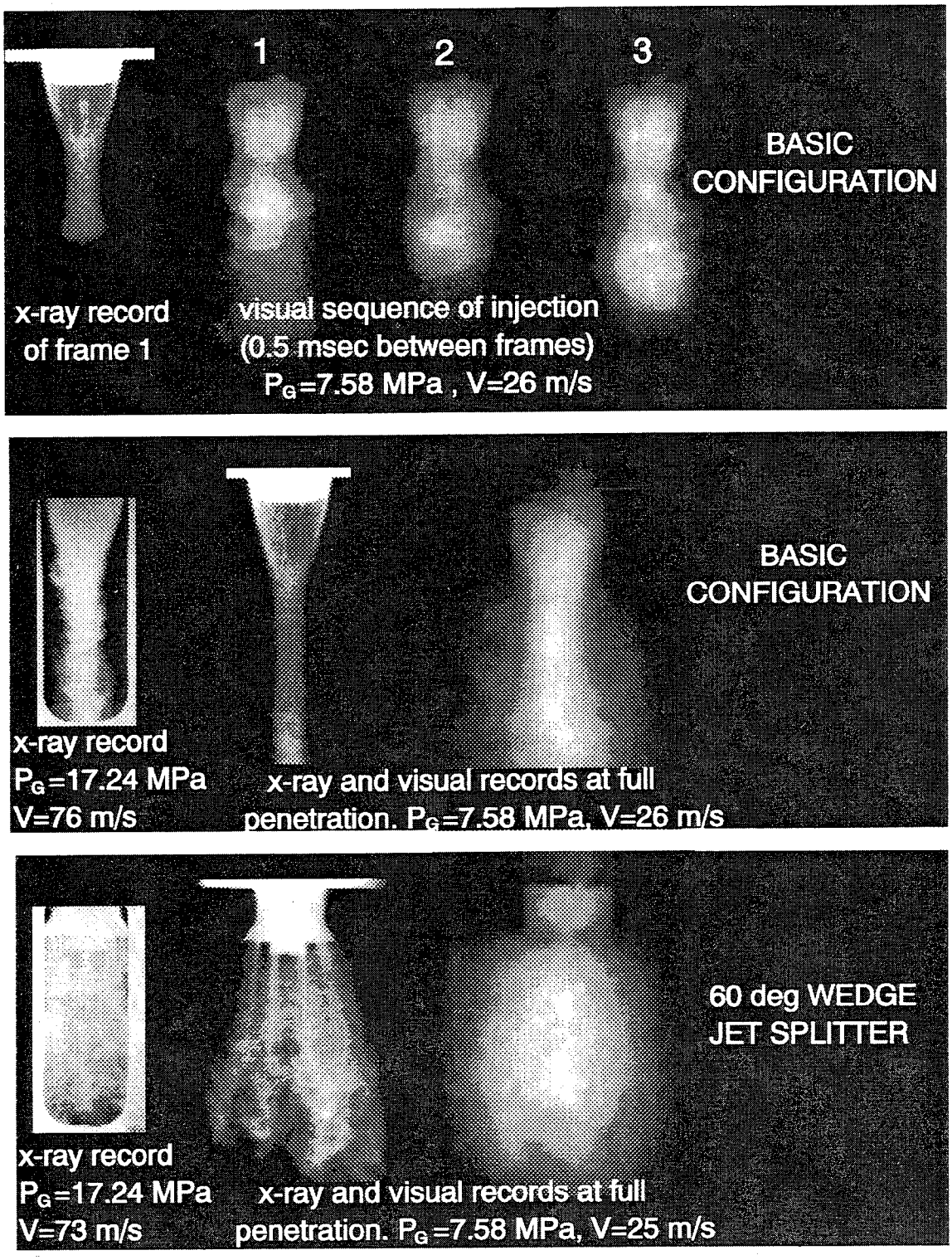

Figure 3. X-ray and visual images of inert jets in main configurations.

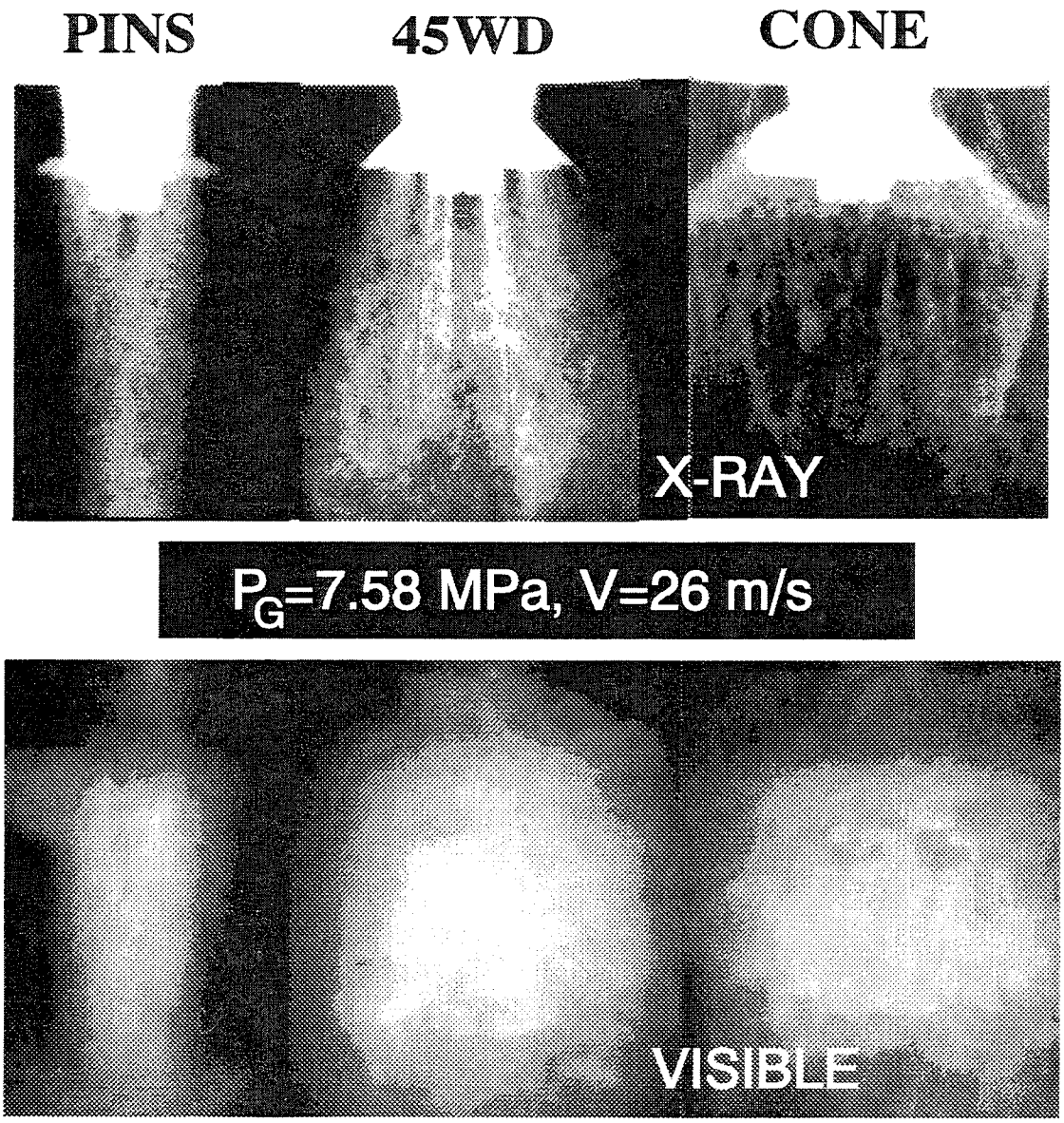

Figure 4. X-ray and visual images of inert jets in ancillary dispersers.

surface of the conical protrusion. Beyond the protrusion, the core collapses toward the chamber centerline, producing longitudinal cylindrical flow. This is also the situation at higher pressure, except that the jet boundaries are less well defined. The images obtained in the 60WD and 45WD tests show that the jet also remains attached to the center protrusion, but is then split and scattered radially outward by the disperser. Significantly, there is no indication of liquid deflection backward from the disperser toward the injector. The images obtained with the PINS resemble those obtained in the basic configuration. The main effect of the PINS is to enhance turbulence in the jet, breaking it into finer ligaments. This effect is more pronounced at low ambient pressures. The images obtained in the CONE configuration show that

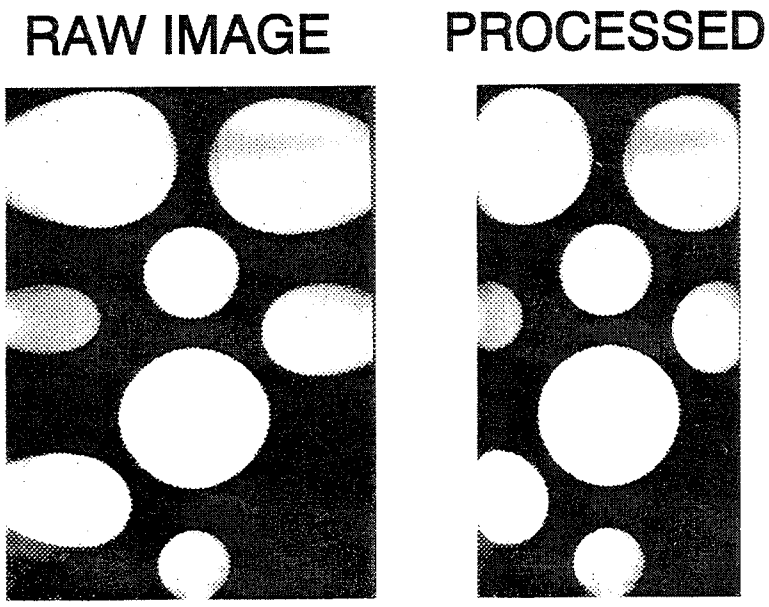

Figure 5. X-ray images of a lead plate with circular holes.

most of the liquid is deflected towards the chamber walls, wetting them. Some of the liquid is scattered backward towards the injector's face. Clearly the "daisy wheel" 45WD and 60WD are the best dispersers. Notably, in the DeSpirito et al. (1994) experiments, the 60WD and 45WD configurations were effective in reducing pressure oscillations, while the PINS was not effective and the CONE actually enhanced the oscillations. Therefore, we concentrated on a daisy wheel disperser in the combustion tests. We chose the 60WD configuration because more of the spray envelope is observable through the chamber windows.

3.2 Combustion Tests. The combustion test parameters and typical injector motion data are shown in Figure 6. The experimental pressure data are summarized in Figures 7 and 8. In all figures, the time is counted from the spark ignition trigger (by a timer sequencer). In all tests, the XM46 was successfully ignited when injection started less than 1 ms before the peak ambient gas combustion pressure. Premature injection (in 1/3 of the tests) resulted in ignition failure. The injection velocities ranged from 105 to 115 m/s.

Several different O_2/H_2/Ar gas mixtures were chosen to determine if mixture stoichiometry influenced the spray combustion dynamics. Mixtures designated A and C are fuel rich, while mixtures B and D

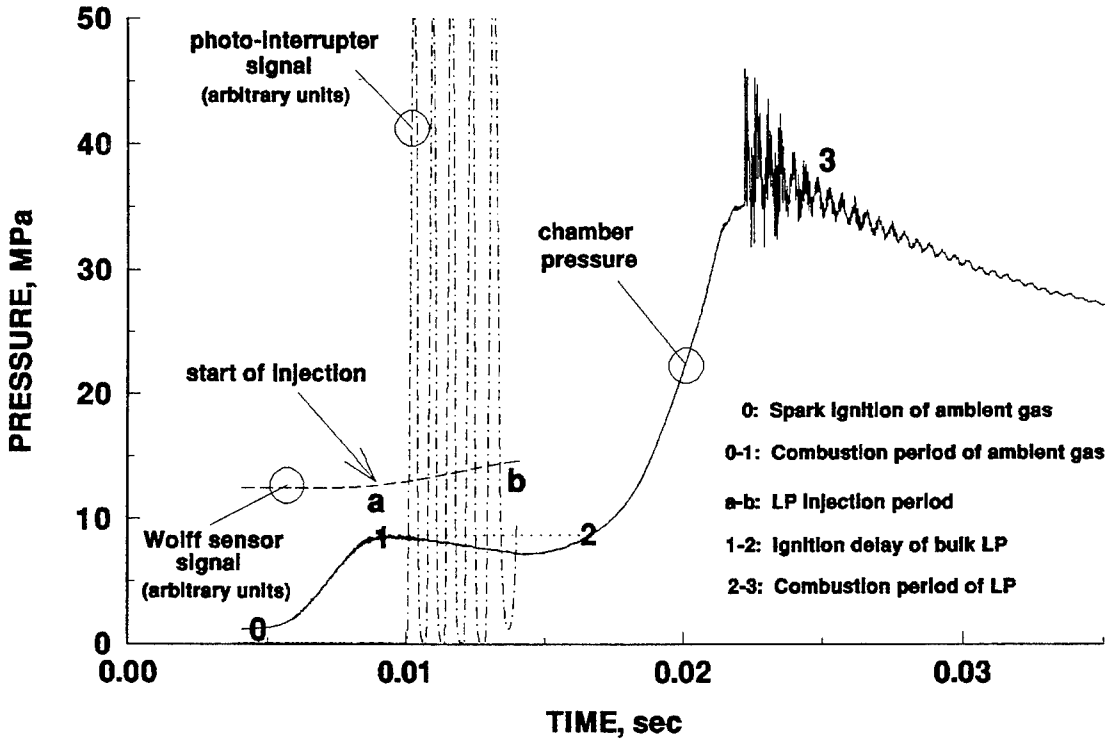

Figure 6. Representative combustion test data.

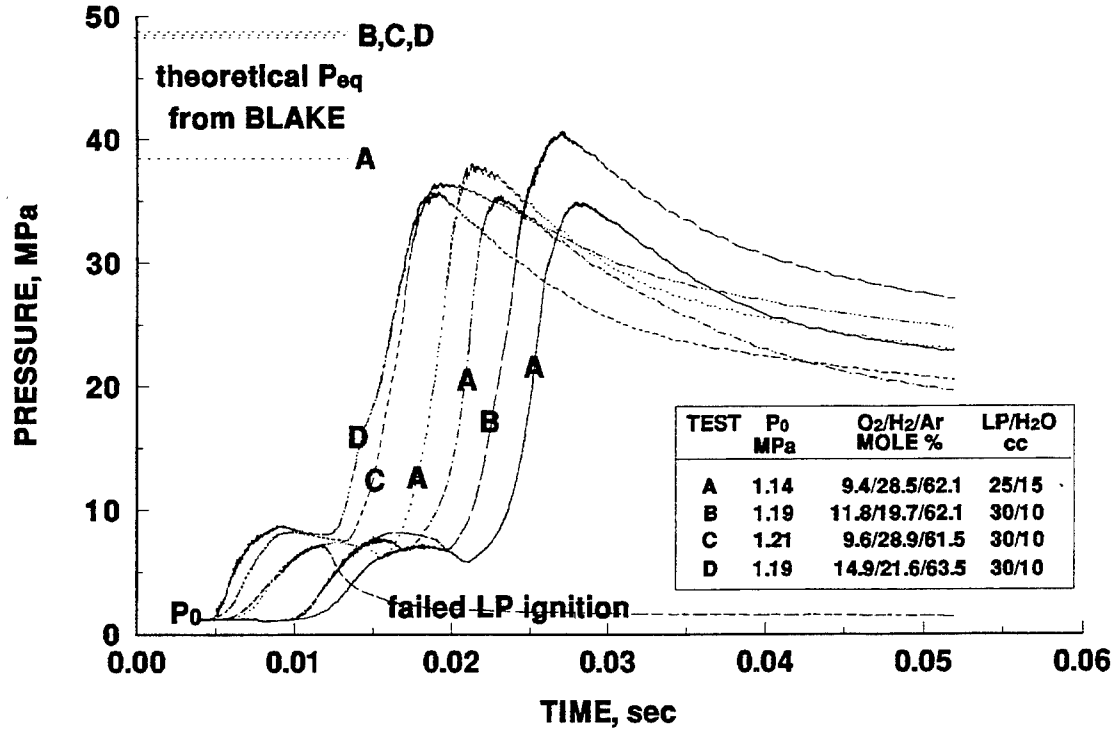

Figure 7. Pressure data of 60WD configuration.

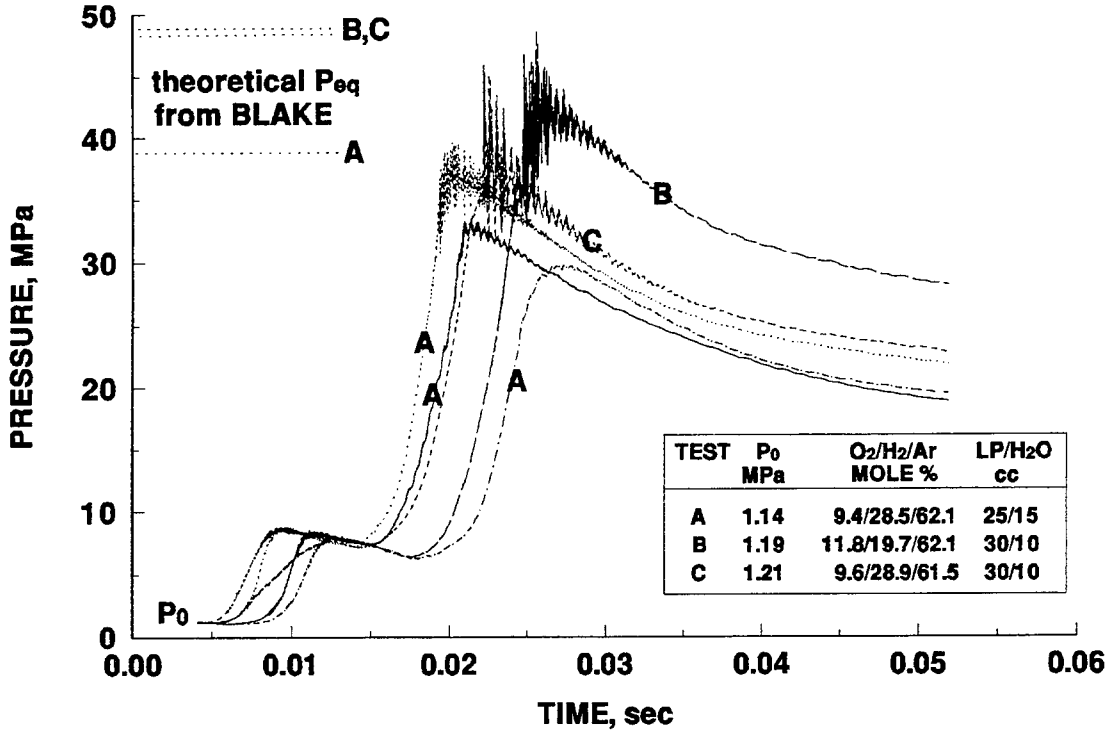

Figure 8. Pressure data of basic configuration.

are fuel lean. Significant deviations from stoichiometry resulted either in failure to ignite the gas or in detonations. Cinematography was only attempted in tests with gas mixture A. The XM46/water mixture employed in conjunction with gas mixture A had a lower energy content than the other tests, and thus was less likely to break the sapphire windows through which the spray was viewed. In tests with the other mixtures, the sapphire windows were replaced with metal blanks.

3.2.1 Thermodynamics. The BLAKE thermodynamic code (Freedman 1982) was used to predict the adiabatic equilibrium states that would be produced by combustion of the various $O_2/H_2/Ar$ - XM46/water combinations. Based on the BLAKE code, combustion of gas mixture A will produce 9.9 MPa, 2,868-K gas. After XM46 is injected, the pressure is predicted to rise to 38 MPa while the temperature drops to 1,572 K. BLAKE predicts that combustion of gas mixture D will produce 10.8 MPa, 3,009-K gas, and that the subsequent combustion of XM46 will further raise the pressure to 48.5 MPa while the temperature drops to about 1,915 K. (The values for mixtures B and C fall between these limits.) As shown in Figures 7 and 8, the measured pressures were 15–20% below the predicted values. This discrepancy is primarily attributable to heat losses. The effect of the amount of water introduced to the chamber following the injection of XM46 was also determined by BLAKE calculations. For example,

if it is assumed that no water is injected in tests in which gas mixture A was employed, a final pressure of 42.8 MPa and temperature of 2,490 K are predicted. Thus, we do not consider that the experimental variation (2 cm^3) in the amount of injected water is significant in interpreting the experimental results.

3.2.2 XM46 Ignition and Combustion. Comparison of the pressure records of failed ignitions to successful ignitions indicates that some of the XM46 ignites promptly upon injection. If ignition were delayed, the pressure would drop precipitously upon injection as the chamber volume expands and heat is transferred to the liquid—just as in the failed ignition tests. However, the pressure is observed to decrease gradually from its initial peak values. Evidence for this prompt energy release is also observed in the cinematic records. Though of poor quality, the records resolve the incipient injector piston motion. Luminosity near the injector face, presumably associated with XM46 combustion, is observed at this early time. Although some combustion does take place during the injection (interval a - b in Figure 6), most of the propellant does not combust until after a delay of nearly 5 ms. During this delay, the injection is completed and the XM46 is dispersed throughout the chamber. The steep rise of the chamber pressure corresponds to the rapid combustion of the dispersed XM46. The only residue in the chamber following these tests was water, indicating that the XM46 burned to completion.

The LP ignition and combustion characteristics corresponding to the two injector configurations tested are summarized in Table 1. Table 1 shows that the (dispersed) XM46 ignition delay was shorter when the 60WD disperser was employed. The pressure rise following ignition was similar (within standard deviation) for both configurations. Differences in the initial composition of the $O_2/H_2/Ar$ mixture had no demonstrable effect on the XM46 combustion characteristics.

Table 1. LP Ignition and Combustion Characteristics

	Mean Ignition Delay (ms)	Standard Deviation (ms)	Mean of Maximum Pressure Gradient (MPa/ms)	Standard Deviation (MPa/ms)	Comments
Basic Configuration	6.34	1.29	8.95	1.62	a
60WD	3.39	0.66	11.16	3.33	b

[a] Large pressure oscillations develop above 30 MPa.
[b] No pressure oscillations.

3.2.3 Pressure Oscillations. The pressure records suggest that the pressure oscillations observed near the peak pressures correspond to the combustion of the last 1 to 3 cm^3 of unburned LP in the chamber. The oscillations have amplitudes of 10 MPa and pressure rise rates in the range of 600–800 MPa/ms. The amplitudes are larger than would be obtained if 3 cm^3 of XM46 were uniformly distributed in the chamber. Such oscillations can arise because of detonations, or due to explosive combustion of concentrated pockets of LP. We do not consider that the oscillations are due to detonation phenomena. (Detonation is associated with supersonic combustion waves.) If the XM46 involved in the oscillations were well distributed throughout the chamber, a detonation wave would have multiplied the already high chamber pressure, resulting in much higher pressure amplitudes than measured. Furthermore, the reactive mixture would likely be diluted below the detonation limit. If the XM46 were concentrated in pockets, its detonation would have yielded local pressures exceeding 500 MPa. Such an event would have damaged the chamber or injector; but no damage was found. We therefore conclude that the oscillations stem from the spontaneous (i.e., explosive) bulk ignition of XM46 blobs which are as large as 1 cm^3. Successive explosive events can generate a train of steep pressure waves with amplitudes in the tens of MPa. The absence of such explosive combustion in the 60WD configuration is attributed to the effectiveness of this configuration in precluding the formation of concentrated pockets of XM46. A measure of this effectiveness can be obtained from Figure 9, which shows cinematic sequences of simulant injection tests in the acrylic chamber. By the end of the injection, the spray in the 60WD configuration is dispersed throughout the chamber volume, while the spray in the basic configuration is still concentrated along the centerline of the chamber. In these tests, the ratio of the densities of the liquid and the ambient gas were similar to those in the combustion tests, thus simulating the main jet breakup and dispersion characteristics. (Helium was chosen in order to provide sufficient ambient pressure for the regenerative injection while maintaining low gas density.)

The mechanism for the explosive combustion is unknown. The data indicate that weak pressure waves develop in the chamber at pressures above 30 MPa in all tests (and with both injector configurations). We speculate that a threshold for a pressure-dependent XM46 reaction is exceeded, and the combustion of the propellant, which is already at an elevated temperature, is explosively accelerated by a pressure wave. A Fast Fourier Transform (FFT) analysis of the pressure traces near peak pressures was performed, and the results are shown in Figure 10. The raw data shown in Figure 10 were filtered at 20 kHz before the FFT operation. This eliminates spurious high frequencies, which stem from nonlinearities and transients in the waves, and [possible] resonance effects due to the stepped mounting of the pressure

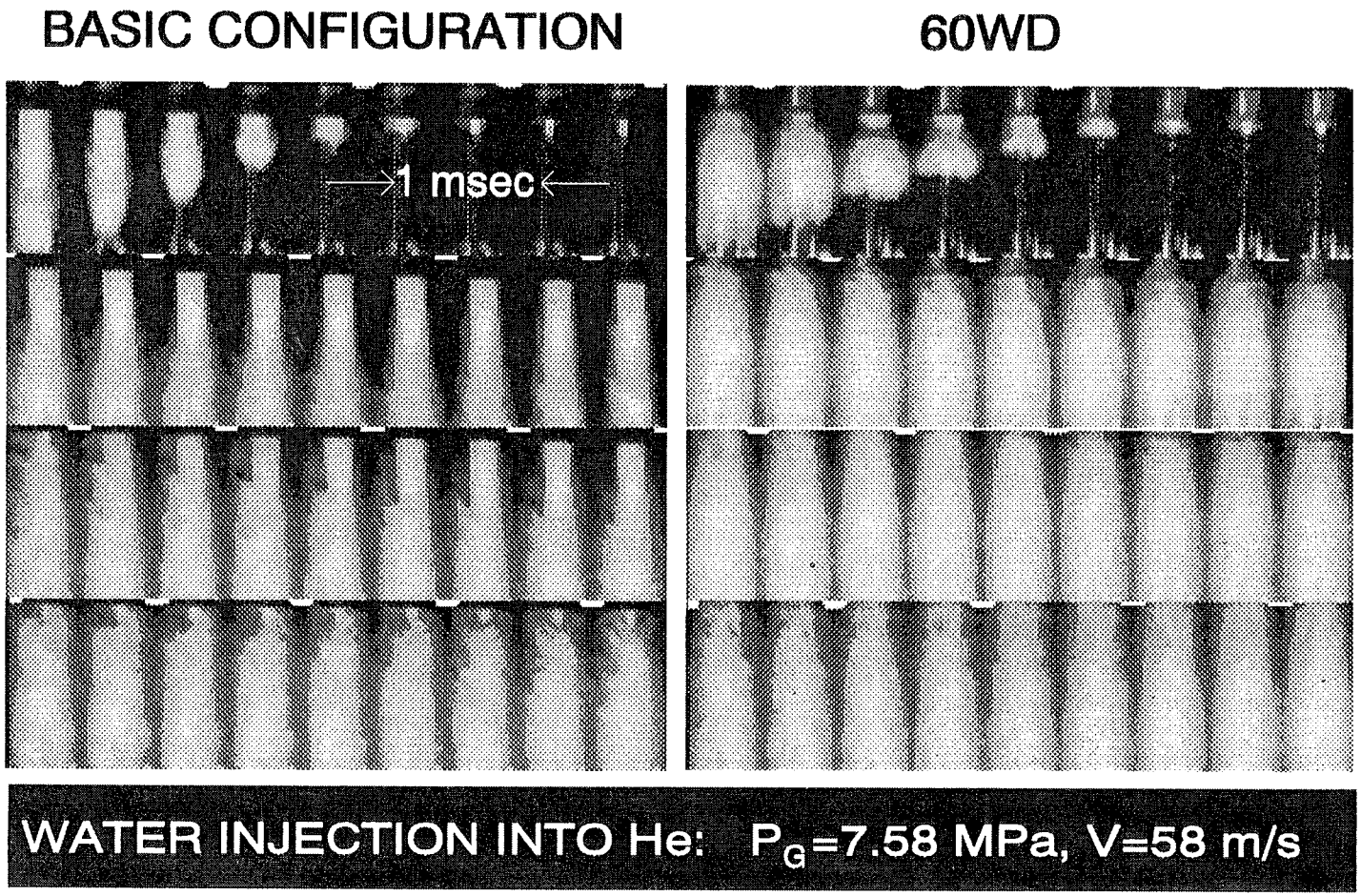

Figure 9. Cinematic sequences of simulant jets.

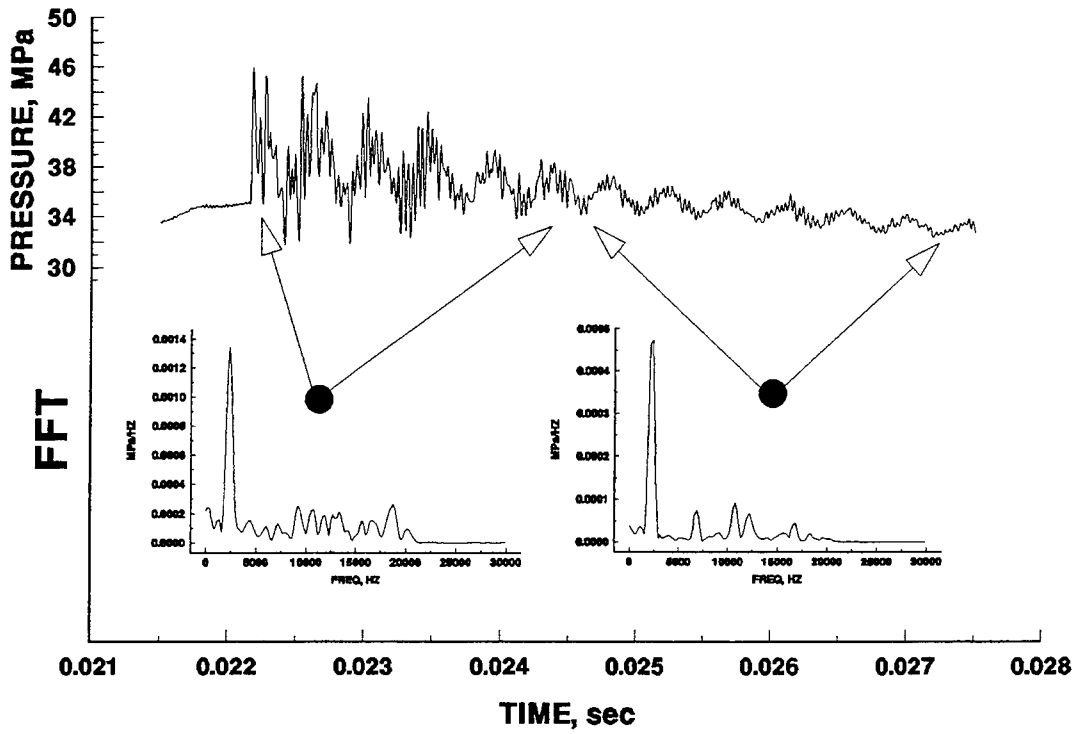

Figure 10. FFT of pressure oscillations.

transducer. The FFT analysis yields a dominant frequency at 2.34 kHz. This frequency is considered to be associated with the fundamental longitudinal acoustic mode of the chamber. During the first 2 ms of the oscillations, there are no discrete frequencies other than the longitudinal mode. The high frequencies are considered to be associated with combustion noise. About 2 ms after the initiation of the oscillations, the combustion is complete, and other discrete frequencies become apparent. These are possibly due to radial and tangential acoustic modes.

It is instructive to compare these pressure oscillations to the oscillations that were obtained when an $O_2/H_2/Ar$ gas mixture transitioned to detonation in a preliminary spark ignition test. Unlike the XM46, the gas mixture can be regarded as perfectly dispersed before ignition. The telltale sign of detonation in a spark-ignited cold gas is the sudden appearance of pressure spikes with values well above P_{eq}. Figure 11 shows the pressure record and its (20-kHz filtered) FFT of the detonator event. Here, a transition to detonation develops at a pressure (3 MPa) when less than 30% of the mixture has reacted. In comparison, when the pressure oscillations develop in the XM46 combustion, more than 80% of the XM46 has burned. The pressure rise rates of the spikes are in the range of 1,000 MPa/ms, about 25%

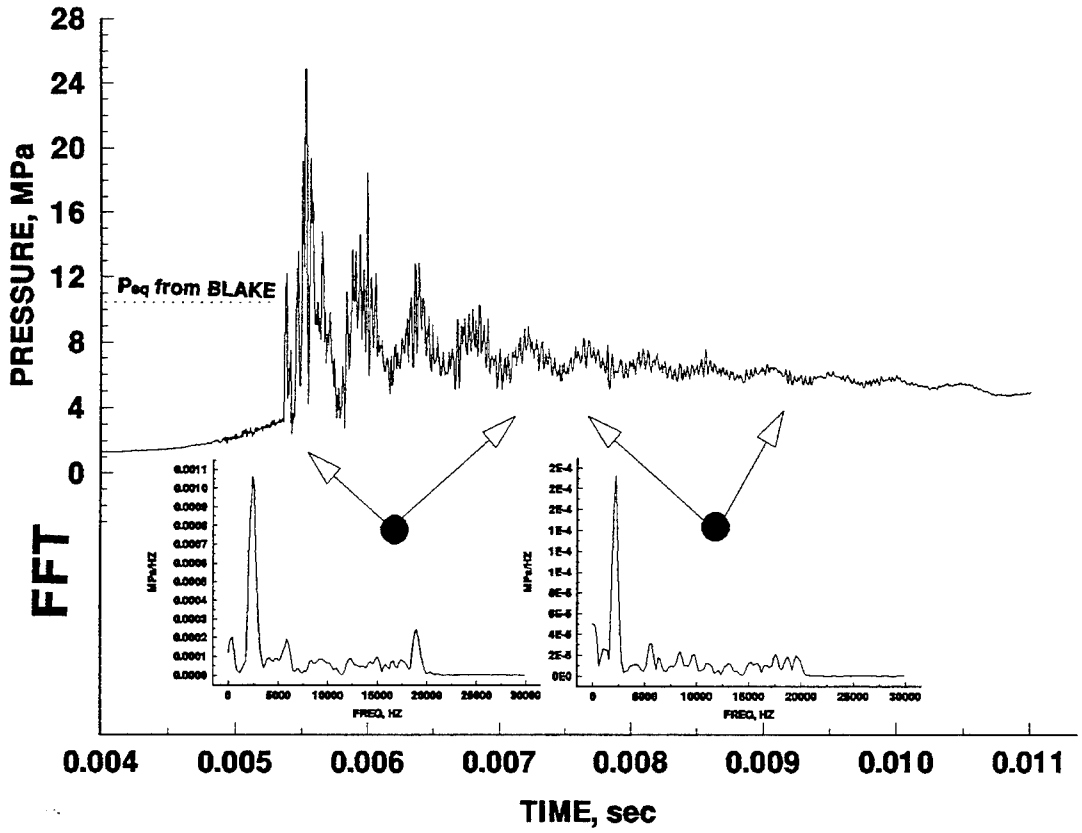

Figure 11. Pressure record of detonative combustion of spark-ignited gas mixture.

larger than those of the XM46 combustion. Subsequent to detonation, acoustic longitudinal waves reverberate in the chamber with the same frequency as in the XM46 combustion. (The sound speeds are comparable in both cases.) Notably, there is less "combustion noise" in the detonative combustion of the gas than in the explosive combustion of the XM46.

4. CONCLUSIONS

The flow structure produced by an injector similar to a practical 30-mm Concept VIC (DeSpirito et al. 1994) injector was successfully imaged using flash x-ray photography. The images show that the liquid (propellant) will remain attached to the wall of the injector's inner piston (i.e., the conical protrusion) in a "basic" Concept VIC configuration. Thus, dispersers attached to the end of the inner piston will be effective in splitting the jet and effecting dispersion radially outward. Moreover, enhanced dispersion is a logical mechanism for reducing pressure oscillations, and therefore, a similar device incorporated into a large caliber RLPG may reduce pressure oscillations. The combustion results also apply to the so called

"puddle" ignition in the 155-mm RLPG. As in our experiments, "puddle" ignition is associated with a dispersed XM46 charge. The present findings indicate that explosive combustion producing pressure spikes can occur at pressures below 50 MPa if poorly dispersed XM46 is ignited by hot gas. This is alarming considering that our experimental ignition pressure profile mimics that of the 155-mm RLPG process.

INTENTIONALLY LEFT BLANK.

5. REFERENCES

Birk, A., and G. Bliesener. "Laboratory Injector for Spray Studies Related to Liquid Propellant Gun." BRL-TR-3209, U.S. Army Ballistic Research Laboratory, February 1991.

Birk, A., and P. Reeves. "Annular Liquid Propellant Jets—Injection, Atomization, and Ignition." BRL-TR-2780, U.S. Army Ballistic Research Laboratory, March 1987.

Birk, A., M. McQuaid, and G. Bliesener. "Reacting Liquid Monopropellant Sprays—Experiments With High Velocity Full Cone Sprays in 33MPa, 500°C Nitrogen." ARL-TR-17, U.S. Army Research Laboratory, December 1992.

Birk, A., M. McQuaid, and M. Gross. "Liquid Core Structure of Evaporating Sprays at High Pressures—Flash X-Ray Studies." 30th JANNAF Combustion Subcommittee Meeting, CPIA Publication 606, vol. 1, pp. 73–85, October 1993.

DeSpirito, J., N. E. Boyer, J. D. Knapton, A. W. Johnson, and R. E. Rychnovsky. "Pressure Oscillation Techniques in a 30-mm Regenerative Liquid Propellant Gun (RLPG)." ARL-TR-437, U.S. Army Research Laboratory, June 1994.

Freedman, E. "BLAKE - A Thermodynamics Code Based on TIGER: User's Guide and Manual." BRL-TR-02411, U.S. Army Ballistic Research Laboratory, July 1982.

INTENTIONALLY LEFT BLANK.

NO. OF COPIES	ORGANIZATION
2	ADMINISTRATOR ATTN DTIC DDA DEFENSE TECHNICAL INFO CTR CAMERON STATION ALEXANDRIA VA 22304-6145
1	DIRECTOR ATTN AMSRL OP SD TA US ARMY RESEARCH LAB 2800 POWDER MILL RD ADELPHI MD 20783-1145
3	DIRECTOR ATTN AMSRL OP SD TL US ARMY RESEARCH LAB 2800 POWDER MILL RD ADELPHI MD 20783-1145
1	DIRECTOR ATTN AMSRL OP SD TP US ARMY RESEARCH LAB 2800 POWDER MILL RD ADELPHI MD 20783-1145
	ABERDEEN PROVING GROUND
5	DIR USARL ATTN AMSRL OP AP L (305)

NO. OF COPIES	ORGANIZATION
1	COMMANDER ATTN SMCAR AEE B D DOWNS USA ARDEC PCTNY ARSNL NJ 07805-5000
2	COMMANDER ATTN SMCAR AEE BR B BRODMAN W SEALS USA ARDEC PCTNY ARSNL NJ 07806-5000
1	COMMANDER ATTN SMCAR AEE W N SLAGG USA ARDEC PCTNY ARSNL NJ 07806-5000
2	COMMANDER ATTN SMCAR AEE A BRACUTI D CHIU USA ARDEC PCTNY ARSNL NJ 07806-5000
4	COMMANDER ATTN SMCAR FSS DA B MACHAK S TRAENDLY C PERAZZO R KOPMAN BLDG 94 USA ARDEC PCTNY ARSNL NJ 07806-5000
2	COMMANDER ATTN SFAE ASM AF A LTC D ELLIS J SHIELDS BLDG 3159 USA ARDEC PCTNY ARSNL NJ 07806-5000
1	COMMANDANT ATTN ATSB CD MLD US ARMY ARMOR CENTER FT KNOX KY 40121
1	COMMANDANT ATTN ATSF TSM CN USAFAS FT SILL OK 78503-5600
2	COMMANDER ATTN AMSMC LSL B KELEBER AMSMC SAS WF G SCHELENKER HS AMCCOM ROCK ISLAND IL 61299-6000
1	DIRECTOR ATTN AMXRO MCS DR D MANN PO BOX 12211 ARMY RESEARCH OFFICE RSRCH TRI PK NC 27709-2211
1	DIRECTOR ATTN AMXRO RT IP LIB SER PO BOX 12211 ARMY RESEARCH OFFICE RSRCH TRI PK NC 27709-2211
1	OLAC PL RKFA ATTN D TALLEY EDWARDS AFB CA 93524
1	CA INST OF TECHNOLOGY ATTN TECHNICAL LIBRARY 4800 OAK GROVE DR JET PROPULSION LAB PASADENA CA 91109-8099
1	THE PENNSYLVANIA STATE UNIVERSITY ATTN PROF K K KUO 140 RESEARCH BLDG, E BIGLER RD UNIV PK PA 16802-7501
1	DIRECTOR ATTN D P MAYNARD J BELLAN 4800 OAK GROVE DR JET PROPULSION LABORATORY CHEMICAL PROCESSES GROUP PROPULSION SYSTEMS SECTION PASADENA CA 91109-8099
1	VEHICLE PROPULSION DIRECTORATE ATTN MS 603 TECHNICAL LIBRARY 21000 BROOKPARK RD NASA LEWIS RESEARCH CENTER CLEVELAND OH 44135-3191

NO. OF COPIES	ORGANIZATION
1	DIRECTOR ATTN R CARLING DIVISION 8357 PO BOX 696 SANDIA NATIONAL LABORATORIES LIVERMORE CA 94551-0969
1	DIRECTOR APPLIED PHYSICS LABORATORY THE JOHNS HOPKINS UNIVERSITY JOHNS HOPKINS RD LAUREL MD 20707
1	PAUL GOUGH ASSOCIATES INC ATTN DR PAUL S GOUGH 1048 SOUTH ST PORTSMOUTH NH 03801-5423
2	JOHNS HOPKINS UNIVERSITY CPIA ATTN T CHRISTIAN TECHNICAL LIBRARY 10630 LITTLE PATUXENT PKWY STE 202 COLUMBIA MD 21042-3200

NO. OF COPIES	ORGANIZATION
	ABERDEEN PROVING GROUND, MD
35	DIR, USARL ATTN: AMSRL WT P A HORST AMSRL WT PA T MINOR T COFFEE G WREN A BIRK (5 CPS) J DE SPIRITO A JUHASZ J KNAPTON C LEVERITT M MCQUAID (5 CPS) B OBERLE P TRAN K WHITE L-M CHANG J COLBURN P CONROY A HORST G KELLER D KOOKER M NUSCA T ROSENBERGER AMSRL WT PB E SCHMIDT AMSRL WT PC R FIFER J VANDERHOFF R BEYER M MILLER AMSRL WT PD B BURNS

INTENTIONALLY LEFT BLANK.

USER EVALUATION SHEET/CHANGE OF ADDRESS

This Laboratory undertakes a continuing effort to improve the quality of the reports it publishes. Your comments/answers to the items/questions below will aid us in our efforts.

1. ARL Report Number ARL-TR-720 Date of Report April 1995

2. Date Report Received _____

3. Does this report satisfy a need? (Comment on purpose, related project, or other area of interest for which the report will be used.) _____

_____

_____

4. Specifically, how is the report being used? (Information source, design data, procedure, source of ideas, etc.)

_____

_____

_____

5. Has the information in this report led to any quantitative savings as far as man-hours or dollars saved, operating costs avoided, or efficiencies achieved, etc? If so, please elaborate. _____

_____

_____

6. General Comments. What do you think should be changed to improve future reports? (Indicate changes to organization, technical content, format, etc.) _____

_____

_____

_____

CURRENT ADDRESS

_____
Organization

_____
Name

_____
Street or P.O. Box No.

_____
City, State, Zip Code

7. If indicating a Change of Address or Address Correction, please provide the Current or Correct address above and the Old or Incorrect address below.

OLD ADDRESS

_____
Organization

_____
Name

_____
Street or P.O. Box No.

_____
City, State, Zip Code

(Remove this sheet, fold as indicated, tape closed, and mail.)

(DO NOT STAPLE)

DEPARTMENT OF THE ARMY

OFFICIAL BUSINESS

NO POSTAGE
NECESSARY
IF MAILED
IN THE
UNITED STATES

BUSINESS REPLY MAIL
FIRST CLASS PERMIT NO 0001,APG,MD

POSTAGE WILL BE PAID BY ADDRESSEE

DIRECTOR
U.S. ARMY RESEARCH LABORATORY
ATTN: AMSRL-WT-PA
ABERDEEN PROVING GROUND, MD 21005-5066